

## FARADAY TOMOGRAPHY WITH LOFAR: NEW PROBE OF THE INTERSTELLAR MAGNETIC FIELD

M. I. R. Alves<sup>1</sup>, V. Jeli <sup>2,3</sup>, K. Ferri re<sup>1</sup> and F. Boulanger<sup>4</sup>

**Abstract.** Magnetic fields are a key constituent of the interstellar medium of our Galaxy. However, their exact role in the Galactic ecosystem is still poorly understood since we do not yet have a complete view of its structure in the Galaxy. This is about to change with the Faraday tomography technique, which allows us to derive the magnetic field in separate regions along the line of sight. We first describe the principle of Faraday tomography and illustrate the power of this novel technique with some of the latest results from the LOW Frequency ARray (LOFAR). We present preliminary results of our LOFAR project, aimed at investigating the origin of the filamentary-like structures revealed by Faraday tomography observations.

Keywords: ISM: general, magnetic fields, structure – radio continuum: ISM – techniques: polarimetric, interferometric

### 1 Introduction

Since interstellar magnetic fields were discovered in our Galaxy (Hall 1949; Hiltner 1949), it has been established that magnetism is pervasive in the Universe. Planets, stars, and galaxies all show the presence of magnetic fields, which span a large range in strength and change considerably in structure. The properties of Galactic interstellar magnetic fields, in different environments and objects, have been inferred throughout the years from a variety of observational methods. These are based on polarization of starlight and dust thermal emission, Zeeman splitting, Faraday rotation, and synchrotron emission (e.g. see reviews by Ferri re 2011; Haverkorn 2015). Not only from observations but also from a theoretical point of view, it became clear that magnetic fields are a vital constituent of the interstellar medium. However, the details of their role in the Galactic ecosystem, for instance in star formation, in the distribution and dynamics of interstellar matter, or in the evolution of supernova remnants, are still poorly known.

A great limitation of most of the aforementioned methods is that they provide line-of-sight integrated quantities, with no details on how the integrands vary along the sightline. Moreover, they probe different components of the magnetic field in different phases of the interstellar medium. For instance, dust polarization (either in emission or extinction) traces the orientation of the plane-of-the-sky magnetic field in the dusty (mostly neutral) medium, while synchrotron emission and its polarization give the same field component but in the general, cosmic-ray filled interstellar medium. The line-of-sight magnetic field can be obtained from Zeeman splitting and Faraday rotation in the neutral and ionized medium, respectively. The key to make progress in studies of Galactic magnetism is thus to combine complementary tracers.

The Faraday tomography method is based on this approach: it relies on a combination of Faraday rotation and synchrotron emission. The observed synchrotron emission from the Galaxy is produced by different regions along the line of sight. The emission produced by each region undergoes Faraday rotation and the amount of rotation increases with distance to the emitting region. The idea is thus to exploit Faraday rotation to locate the different regions along the line of sight. Moreover, the amount of Faraday rotation increases with wavelength squared ( $\lambda^2$ ). Therefore, observing at large wavelengths, or low frequencies, is very efficient to

<sup>1</sup> IRAP, Universit  de Toulouse, CNRS, 9 avenue du Colonel Roche, BP 44346, 31028, Toulouse Cedex 4, France

<sup>2</sup> Ruđer Boškovi  Institute, Bijeni ka cesta 54, 10000 Zagreb, Croatia

<sup>3</sup> ASTRON - The Netherlands Institute for Radio Astronomy, PO Box 2, 7990 AA Dwingeloo, The Netherlands

<sup>4</sup> IAS, Universit  Paris-Sud 11, CNRS, B timent 121, 91405 Orsay, France

probe the nearby interstellar medium in detail. On the other hand, observations at smaller wavelengths are more suitable to probe the interstellar medium over large distances. Faraday tomography is being increasingly used, thanks to the high-quality data, with wide wavelength coverage and high angular resolution, provided by recent radio telescopes such as the LOw Frequency ARray (LOFAR). The few studies available for various sightlines reveal a rich interstellar medium, filled with a number of synchrotron emitting regions interspersed with Faraday rotating screens (e.g. Iacobelli et al. 2013; Jelić et al. 2014, 2015).

## 2 Faraday tomography

Faraday tomography exploits the Faraday rotation of synchrotron polarized emission. The amount of Faraday rotation of the polarized emission produced at a point P with line of sight depth  $L$  is equal to the wavelength squared times the Faraday depth ( $\phi$ ) of point P. The latter is proportional to the line-of-sight integral of the free-electron density times the line-of-sight magnetic field ( $\phi = \int_0^L n_e B_{||} dz$ ). The synchrotron emissivity at a given wavelength is a function of the plane-of-the-sky magnetic field ( $\vec{B}_{\perp}$ ) times the density of cosmic-ray electrons. Essentially, one measures the synchrotron polarized intensity at a large number of different wavelengths and converts its variation with  $\lambda^2$  into a variation with  $\phi$  (alike a Fourier transform, Brentjens & de Bruyn 2005).

Consider a line of sight that intersects four interstellar clouds, as Fig. 1 depicts: two Faraday-rotating (light grey) and two synchrotron-emitting (dark blue) clouds. The top panel shows how these are located as a function of distance from the observer,  $z$ , placed at the far left. The red arrows give the direction of the magnetic field in each Faraday-rotating cloud. As per the above equation,  $\phi$  increases or decreases across the rotating clouds according to whether the magnetic field points towards or away from the observer. This is illustrated in the middle panel, which shows the variation of  $\phi$  with  $z$ :  $\phi_1$  corresponds to the Faraday thickness of the closer Faraday-rotating cloud and  $\phi_2$  is the cumulated Faraday thickness of both Faraday-rotating clouds. The bottom panel shows the Faraday spectrum,  $|F(\phi)|$ , where the two peaks at  $\phi_1$  and  $\phi_2$  represent the polarized emission from the closer and the farther synchrotron-emitting clouds, respectively. In Fig. 1-left the Faraday-rotating and the synchrotron-emitting clouds are spatially separated; in Fig. 1-right the closer synchrotron-emitting cloud is embedded in the closer Faraday-rotating cloud, and hence it has a finite Faraday thickness that extends over a range of Faraday depths (up to nearly  $\phi_1$ ). Regions that are extended in  $\phi$  are called Faraday thick. However, this definition is wavelength dependent and in practice the shape of the Faraday spectrum depends on the instrument's wavelength coverage and resolution (Brentjens & de Bruyn 2005).

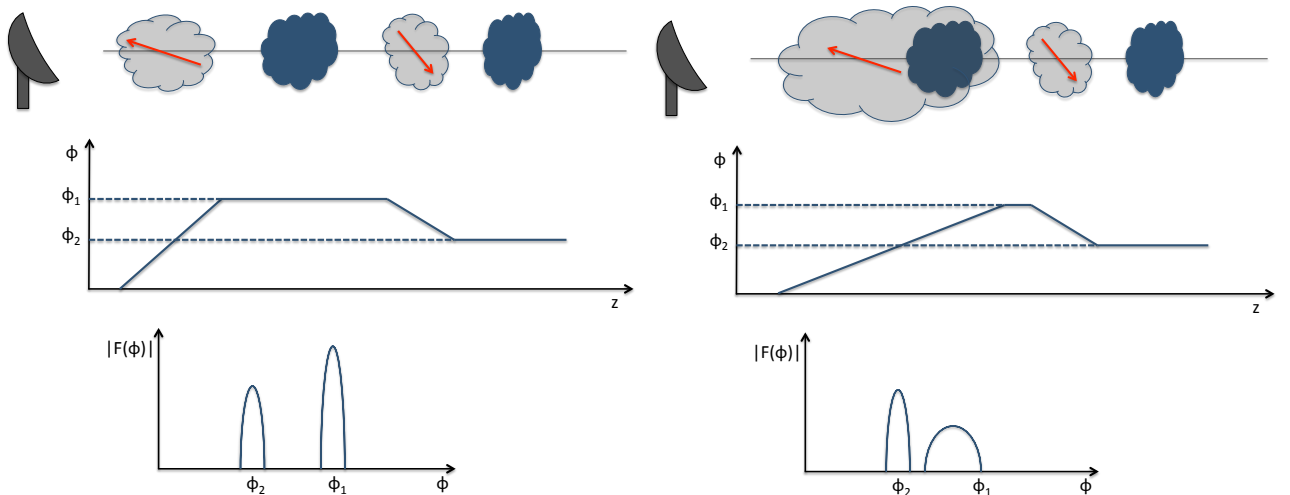


**Fig. 1.** Illustration of the principle of Faraday tomography. See main text for details. **Left:** The Faraday-rotating clouds (light grey) and the synchrotron-emitting clouds (dark blue) are spatially separated. **Right:** The closer synchrotron-emitting cloud is embedded in the closer Faraday-rotating cloud.

In practice one applies the technique to all the lines of sight in a given field, obtaining a Faraday depth cube: synchrotron polarized intensity as a function of position-position-Faraday depth, or  $\alpha - \delta - \phi$ . The challenge consists in identifying the structures detected in the Faraday depth cube with physical structures in the interstellar medium for which we know the position in real space,  $\alpha - \delta - z$  (from e.g. HI and H $\alpha$  line

observations, dust extinction measurements from stellar reddening). If such a correlation is found then we can derive (i) the intensity and orientation of  $\vec{B}_\perp$  from the synchrotron polarized intensity and (ii) the mean line-of-sight magnetic field  $\vec{B}_\parallel$  in the ionized regions from their Faraday depth. Or, as is often the case, the structures seen in the Faraday cube reveal the presence of Faraday screens located in front of the background Galactic synchrotron emission, which is then displaced in Faraday depth  $\phi$  (Sect. 3.1). In this case, we can measure the Faraday thickness,  $\Delta\phi$ , of the structure and estimate its mean  $\vec{B}_\parallel$ .

### 3 Towards the physical properties of ‘‘Faraday filaments’’

#### 3.1 The richness of Faraday tomography

Recent LOFAR Faraday depth cubes revealed a bewildering variety of structures in the interstellar medium. In particular, long and linear features that are likely associated with physical structures of ionized gas. A prominent example is the  $4^\circ$  long and  $7.5'$  wide straight filamentary feature detected in a high Galactic latitude field centred on the quasar 3C196 (labelled A in Fig. 2, Jelić et al. 2015). Figure 2 shows the polarized intensity of the different structures seen at distinct Faraday depths, between  $-3$  and  $+5$   $\text{rad}/\text{m}^2$ , in the 3C196 field. Structure A (in orange) is a perfect example of a Faraday screen, mentioned above: it displaces the background synchrotron emission (in purple) from  $\phi \simeq +2$   $\text{rad}/\text{m}^2$ , where it leaves a hole, to lower Faraday depths of about  $+0.5$   $\text{rad}/\text{m}^2$ . The Faraday thickness of structure A is thus  $1.5$   $\text{rad}/\text{m}^2$ . Since this feature is not seen in the total intensity maps nor in the currently available H $\alpha$  surveys (typical tracer of ionized gas), which do not have the angular resolution to reveal such a narrow structure, it is hard to determine its physical properties (e.g. distance and free-electron density). Consequently, Jelić et al. (2015) could only use the measured Faraday thickness to place lower limits in the product  $n_e B_\parallel$ . Assuming that feature A is indeed a filament and is located nearby, say within 200 pc (it is unlikely located much beyond this distance, given its large angular size), Jelić et al. estimated a path length  $ds = 0.3$  pc. As a result,  $n_e B_\parallel > 6.2$   $\text{cm}^{-3} \mu\text{G}$  in this Faraday, filamentary, screen.

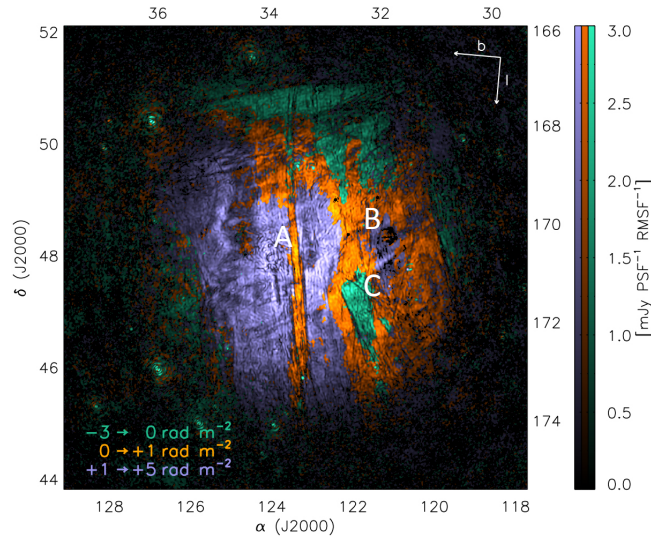


**Fig. 2.** The polarized intensity at different Faraday depth intervals, as indicated in the figure, in the LOFAR 3C196 observations of Jelić et al. (2015). The labels A, B, and C identify noticeable structures in the field.

The primary question that arises from this study is: what is the origin of such filaments that are (so far) only seen in Faraday rotation? To explore their origin we need to know their physical properties, i.e., to associate them with physical structures in the interstellar medium. Indeed, filaments of similar sizes to those detected in Faraday tomography studies are found in HI and H $\alpha$  observations of the interstellar medium (e.g. McCullough & Benjamin 2001; Clark et al. 2014). We are currently carrying out different observational projects with LOFAR, with the goal of investigating the possible connection between ‘‘Faraday filaments’’ and interstellar filaments.

#### 3.2 The McCullough & Benjamin interstellar filament

We selected a narrow ( $20''$ ) and long ( $2^\circ$ ) filament of ionized gas detected serendipitously in high-resolution H $\alpha$  observations by McCullough & Benjamin (2001) to perform Faraday tomography with LOFAR. From the

observed  $H\alpha$  intensity of 0.5 R we can estimate its free-electron density, for a given electron temperature and size. Assuming a typical electron temperature of  $10^4$  K, that the filament is cylindrical and located within 200 pc (as suggested by its radial velocity), we obtain an electron density of  $2 \text{ cm}^{-3}$ . Further assuming a typical magnetic field strength in the ionized gas of  $0.5\text{--}2 \mu\text{G}$ , yields a Faraday thickness of  $0.3\text{--}1.1 \text{ rad/m}^2$  for the filament. This is similar to the Faraday thickness of filament A in the LOFAR observations of Jelić et al. (2015).

We used the LOFAR high-band antennas to measure the polarization, between 115 and 175 MHz, of a  $\sim 5^\circ \times 5^\circ$  region of the sky centred on the McCullough & Benjamin interstellar filament, at  $(l, b) \simeq (140^\circ, 38^\circ)$ . After a first data reduction iteration, we produced the Faraday depth cube that covers  $\phi = [-40, 40] \text{ rad/m}^2$  in steps of  $0.25 \text{ rad/m}^2$ . While no signature of the filament is seen, we do detect diffuse polarized emission across the field at high (and negative) Faraday depths,  $\phi \sim -33$  to  $-28 \text{ rad/m}^2$ . We are currently re-processing the LOFAR observations to produce a higher angular resolution Faraday depth cube (better than the present  $3'$ ).

If we do detect the  $H\alpha$  filament in the Faraday depth cube, it will represent the first association between a LOFAR Faraday filament and a gaseous structure in the interstellar medium. We will then be able to estimate its magnetic field, combining LOFAR with the ancillary  $H\alpha$  observations. In the case of a non-detection, we will give lower limits on the filament's magnetic field. The results will allow us to examine the possible formation scenarios of this structure. McCullough & Benjamin (2001) argue that the most probable origin of the filament is an ionized trail left by photoionization from a star or a compact object, which would also explain its straightness. The authors also consider the possibility that this is an unusual linear filament associated with a large-scale nearby bubble. Indeed, observational and numerical studies (e.g. Planck Collaboration Int. XXXII. 2016; Hennebelle 2013) have shown that interstellar filaments can be formed from turbulent motions in the atomic medium, which stretch/compress the gas into filaments or sheets, thereby stretching/compressing the magnetic field in the same direction. The magnetic field structure is thus a clue to the filament's origin.

## 4 Conclusions

Faraday tomography is proving to be a powerful technique for Galactic magnetism studies. Its main asset is the capability to probe the magnetic field in different regions along the line of sight. LOFAR Faraday tomography studies have started to provide new views into the structure of the interstellar medium, although still incomplete and puzzling. Notably, the detection of long and narrow filamentary structures that are most likely associated with physical structures of ionized gas. Still, it has not yet been possible to establish a connection between, what we name, "Faraday filaments" and gaseous filaments in the interstellar medium. This is precisely the goal of our LOFAR project in which we perform Faraday tomography of a region of the sky that contains an interstellar filament of ionized gas, seen in  $H\alpha$  observations. The data are currently being analysed.

M.I.R. Alves acknowledges the support by the Centre National d'Études Spatiales (CNES postdoctoral fellowship). LOFAR, the Low Frequency Array designed and constructed by ASTRON, has facilities in several countries, that are owned by various parties (each with their own funding sources), and that are collectively operated by the International LOFAR Telescope (ILT) foundation under a joint scientific policy.

## References

- Brentjens, M. A. & de Bruyn, A. G. 2005, *A&A*, 441, 1217  
 Clark, S. E., Peek, J. E. G., & Putman, M. E. 2014, *ApJ*, 789, 82  
 Ferrière, K. 2011, *Mem. Soc. Astron. Italiana*, 82, 824  
 Hall, J. S. 1949, *Science*, 109, 166  
 Haverkorn, M. 2015, in *Astrophysics and Space Science Library*, Vol. 407, *Magnetic Fields in Diffuse Media*, ed. A. Lazarian, E. M. de Gouveia Dal Pino, & C. Melioli, 483  
 Hennebelle, P. 2013, *A&A*, 556, A153  
 Hiltner, W. A. 1949, *ApJ*, 109, 471  
 Iacobelli, M., Haverkorn, M., & Katgert, P. 2013, *A&A*, 549, A56  
 Jelić, V., de Bruyn, A. G., Mevius, M., et al. 2014, *A&A*, 568, A101  
 Jelić, V., de Bruyn, A. G., Pandey, V. N., et al. 2015, *A&A*, 583, A137  
 McCullough, P. R. & Benjamin, R. A. 2001, *AJ*, 122, 1500  
 Planck Collaboration Int. XXXII. 2016, *A&A*, 586, A135